RG flow of projectable Hořava gravity in 3+1 dimensions

Alexander Kurov

Lebedev Physics Institute

Problems of the Modern Mathematical Physics 2025

12 February, Dubna

In collaboration with A. O. Barvinsky and S. M. Sibiryakov

Motivation for Hořava gravity

Einstein GR

$$S_{EH} = \frac{M_P^2}{2}\int dt\, d^dx\, \sqrt{-g}R \quad \Rightarrow \quad \frac{M_P^2}{2}\int dt\, d^dx\, \left(h_{ij}\Box h^{ij} + \dots\right) \qquad (1)$$

Higher derivative gravity (Stelle 1977)

$$\int \left(R + R^2 + R_{\mu\nu}R^{\mu\nu}\right) \quad \Rightarrow \quad \int \left(h_{ij}\Box h^{ij} + h_{ij}\Box^2 h^{ij} + \dots\right) \qquad (2)$$

The theory is renormalizable and asymptotically free. However the theory is not unitary due to presence of ghosts.

Hořava gravity (2009)

The key is the anisotropic scaling of time and space coordinates,

$$t \mapsto b^{-d} t \,, \quad x^i \mapsto b^{-1} x^i \,, \qquad i = 1, \ldots, d \tag{3}$$

The theory contains only second time derivatives

$$\int \underbrace{dt\, d^d x}_{\propto b^{-2d}} \left(\dot{h}_{ij} \dot{h}_{ij} - h_{ij} (-\Delta)^d h_{ij} + \ldots \right) \tag{4}$$

Foliation preserving diffeomorphisms

$$t \mapsto t'(t) \,, \qquad x^i \mapsto x'^i(t, \mathbf{x}) \tag{5}$$

Metric decomposition

The metric in the action of HG is expanded into the lapse N, the shift N^i and the spatial metric γ_{ij} like in the Arnowitt–Deser–Misner (ADM) decomposition,

$$\mathrm{d}s^2 = N^2\mathrm{d}t^2 - \gamma_{ij}(\mathrm{d}x^i + N^i\mathrm{d}t)(\mathrm{d}x^j + N^j\mathrm{d}t)\,. \tag{6}$$

Fields are assigned the following dimensions under the anisotropic scaling:

$$[N] = [\gamma_{ij}] = 0\,, \qquad [N^i] = d - 1\,. \tag{7}$$

Projectable version

A.Barvinsky, D.Blas, M.Herrero-Valea, S.Sibiryakov, C.Steinwachs (2016)

We consider *projectable* version of Hořava gravity. The lapse N is restricted to be a function of time only, $N = N(t)$

$$S = \frac{1}{2G}\int \mathrm{d}t\, \mathrm{d}^d x \sqrt{\gamma}\big(K_{ij}K^{ij} - \lambda K^2 - \mathcal{V}\big)\ , \tag{8}$$

where

$$K_{ij} = \frac{1}{2}\left(\dot{\gamma}_{ij} - \nabla_i N_j - \nabla_j N_i\right)\ . \tag{9}$$

The potential part $\mathcal{V}$ in $d = 3$ reads,

$$\begin{aligned}\mathcal{V} =& 2\Lambda - \eta R + \mu_1 R^2 + \mu_2 R_{ij}R^{ij} \\ &+ \nu_1 R^3 + \nu_2 R R_{ij}R^{ij} + \nu_3 R^i_j R^j_k R^k_i + \nu_4 \nabla_i R \nabla^i R + \nu_5 \nabla_i R_{jk} \nabla^i R^{jk}\ ,\end{aligned} \tag{10}$$

This expression includes all relevant and marginal terms. It contains 9 couplings $\Lambda, \eta, \mu_1, \mu_2$ and $\nu_a, a = 1, \ldots, 5$.

Dispersion relations and Lorentz violation scale

The spectrum of perturbations contains a transverse-traceless graviton and a scalar mode. Both modes have positive kinetic terms when G is positive and

$$\lambda < 1/3 \quad \text{or} \quad \lambda > 1 \,. \tag{11}$$

Their dispersion relations around a flat background are

$$\omega_{tt}^2 = \eta k^2 + \mu_2 k^4 + \nu_5 k^6 \,, \tag{12a}$$

$$\omega_s^2 = \frac{1-\lambda}{1-3\lambda}\big(-\eta k^2 + (8\mu_1 + 3\mu_2)k^4\big) + \nu_s k^6 \,, \tag{12b}$$

where k is the spatial momentum and we have defined

$$\nu_s \equiv \frac{(1-\lambda)(8\nu_4 + 3\nu_5)}{1-3\lambda} \,. \tag{13}$$

These dispersion relations are problematic at low energies where they are dominated by the k^2-terms.
We see that (12a) exhibits a transition between $\omega_{tt} \propto k^3$ at large k and $\omega_{tt} \propto k$ at small momenta. The transition happens at the momentum

$$k = M_{LV} \sim \nu_5^{-1/4} \,. \tag{14}$$

Essential couplings

Background effective action Γ_{eff} depends on the choice of gauge fixing

$$\Gamma_{\text{eff}} \mapsto \Gamma_{\text{eff}} + \epsilon \mathcal{A}, \tag{15}$$

where $\mathcal{A}$ is a linear combination of equations of motion.
The UV behavior of the theory is parameterized by seven couplings G, λ, ν_a, $a = 1, \ldots, 5$. The essential couplings can be chosen as follows,

$$\mathcal{G} = \frac{G}{\sqrt{\nu_5}}, \qquad \lambda, \qquad u_s = \sqrt{\frac{\nu_s}{\nu_5}}, \qquad v_a = \frac{\nu_a}{\nu_5}, \quad a = 1, 2, 3. \tag{16}$$

The one-loop β-function of λ depends only on the first three of these couplings and reads,

$$\beta_\lambda = \mathcal{G} \frac{27(1-\lambda)^2 + 3u_s(11-3\lambda)(1-\lambda) - 2u_s^2(1-3\lambda)^2}{120\pi^2(1-\lambda)(1+u_s)u_s} \,. \tag{17}$$

The gauge-dependent β-function of G (not $\mathcal{G}$) was also computed.

A.Barvinsky, M.Herrero-Valea, S.Sibiryakov (2019)

Beta functions

Essential couplings

$$\mathcal{G} = \frac{G}{\sqrt{\nu_5}}, \qquad \lambda, \qquad u_s = \sqrt{\frac{(1-\lambda)(8\nu_4+3\nu_5)}{(1-3\lambda)\nu_5}}, \qquad v_a = \frac{\nu_a}{\nu_5}, \quad a = 1,2,3, \tag{18}$$

$$\beta_\lambda = \mathcal{G}\frac{27(1-\lambda)^2 + 3u_s(11-3\lambda)(1-\lambda) - 2u_s^2(1-3\lambda)^2}{120\pi^2(1-\lambda)(1+u_s)u_s} + O(\mathcal{G}^2), \tag{19a}$$

$$\beta_\mathcal{G} = \frac{\mathcal{G}^2}{26880\pi^2(1-\lambda)^2(1-3\lambda)^2(1+u_s)^3u_s^3}\sum_{n=0}^{7} u_s^n\,\mathcal{P}_n^\mathcal{G}[\lambda, v_1, v_2, v_3] + O(\mathcal{G}^3), \tag{19b}$$

$$\beta_\chi = A_\chi\frac{\mathcal{G}}{26880\pi^2(1-\lambda)^3(1-3\lambda)^3(1+u_s)^3u_s^5}\sum_{n=0}^{9} u_s^n\,\mathcal{P}_n^\chi[\lambda, v_1, v_2, v_3] + O(\mathcal{G}^2), \tag{19c}$$

where the prefactor coefficients $A_\chi = (A_{u_s}, A_{v_1}, A_{v_2}, A_{v_3})$ equal

$$A_{u_s} = u_s(1-\lambda), \quad A_{v_1} = 1, \quad A_{v_2} = A_{v_3} = 2. \tag{20}$$

Example of a polynomial

$$\begin{aligned}\mathcal{P}_2^{u_s} = -2(1-\lambda)^3\big[&2419200v_1^2(1-\lambda)^2 + 8v_2^2(42645\lambda^2 - 86482\lambda + 43837)\\ &+ v_3^2(58698 - 106947\lambda + 48249\lambda^2) + 4032v_1\big(462v_2(1-\lambda)^2 + 201v_3(1-\lambda)^2\\ &+ 30\lambda^2 - 44\lambda - 10\big) + 8v_2(6252\lambda^2 - 9188\lambda - 1468) + 8v_2v_3(34335\lambda^2 - 71196\lambda\\ &+ 36861) + v_3(20556\lambda^2 - 30792\lambda - 3696) + 4533\lambda^2 - 3881\lambda + 1448\big].\end{aligned}$$

Fixed points of RG flow

There are 5 solutions for the system of equations

$$\beta_{g_i}/\mathcal{G} = 0\ , \qquad g_i = \lambda, u_s, v_1, v_2, v_3\ . \tag{21}$$

They written down in the table

λ	u_s	v_1	v_2	v_3	$\beta_{\mathcal{G}}/\mathcal{G}^2$	AF?
0.1787	60.57	-928.4	-6.206	-1.711	-0.1416	yes
0.2773	390.6	-19.88	-12.45	2.341	-0.2180	yes
0.3288	54533	3.798×10^{8}	-48.66	4.736	-0.8484	yes
0.3289	57317	-4.125×10^{8}	-49.17	4.734	-0.8784	yes
0.333332	3.528×10^{11}	-6.595×10^{23}	-1.950×10^{8}	4.667	-3.989×10^{6}	yes

Invariance of GR under 4d diffeomorphisms sets the value of λ to 1. That's why one expects that $\lambda \to 1^+$ in the IR limit. However, all the solutions lie on the left side of the unitary domain

$$\lambda < 1/3 \quad \text{or} \quad \lambda > 1 \tag{22}$$

and there are no RG trajectories with $\lambda \to 1^+$.

$\lambda \to \infty$ limit

A.Gümrükçüoğlu and S.Mukohyama, Rev. D 83 (2011) 124033

The beta function β_λ diverges in the limit $\lambda \to \infty$. For the new variable ϱ, the limit $\lambda = \infty$ corresponds to the finite $\varrho = 1$. It's beta function reads

$$\beta_\varrho = 3(1-\varrho)\mathcal{G}\frac{2u_s^2 + u_s\varrho(4-5\varrho) - 3\varrho^2}{40\pi^2 u_s(1+u_s)\varrho}, \quad \varrho \equiv 3\frac{1-\lambda}{1-3\lambda}. \tag{23}$$

Solutions of the system

$$\beta_\chi/\mathcal{G}\Big|_{\substack{\lambda=\infty \\ (\varrho=1)}} = 0\ , \qquad \chi = u_s, v_1, v_2, v_3\ . \tag{24}$$

are written down in the table

№	u_s	v_1	v_2	v_3	$\beta_\mathcal{G}/\mathcal{G}^2$	AF?	Can flow out of $\varrho = 1$?
1	0.0195	0.4994	-2.498	2.999	-0.2004	yes	no
2	0.0418	-0.01237	-0.4204	1.321	-1.144	yes	no
3	0.0553	-0.2266	0.4136	0.7177	-1.079	yes	no
4	12.28	-215.1	-6.007	-2.210	-0.1267	yes	yes
5 (A)	21.60	-17.22	-11.43	1.855	-0.1936	yes	yes
6 (B)	440.4	-13566	-2.467	2.967	0.05822	no	yes
7	571.9	-9.401	13.50	-18.25	-0.0745	yes	yes
8	950.6	-61.35	11.86	3.064	0.4237	no	yes

Stability matrix

In the vicinity of a fixed point, the linearized RG flow can be analyzed with the help of the stability matrix $B_i{}^j$,

$$\tilde{\beta}_{g_i} \cong \sum_j B_i{}^j (g_j - g_j^*), \quad B_i{}^j \equiv \left(\frac{\partial \tilde{\beta}_{g_i}}{\partial g_j} \right) \Big|_{g_i = g_i^*}, \quad \tilde{\beta}_{g_i} = \beta_{g_i} / \mathcal{G}, \tag{25}$$

where g_i^* are fixed point values of the coupling constants.

№	λ	θ_1	θ_2	θ_3	θ_4	θ_5
1	0.1787	-0.3416	-0.06495	0.002639	$0.1902 \pm 0.1760\, i$	
2	0.2773	-0.06504	0.001944	0.02859	0.2647	0.2751

Table: Eigenvalues θ^I of the stability matrix for the first two fixed points with finite λ.

RG equation

We choose as an initial condition of the RG equation a point slightly shifted from the fixed point g^* in the repulsive direction

$$\begin{cases} \dfrac{dg_i}{d\tau} = \tilde{\beta}_{g_i}, \quad g_i = (v_1, v_2, v_3, u_s, \lambda \text{ or } \varrho), \\ g_i(0) = g_i^* + \varepsilon\, c_J\, w_i^J, \quad J = 1, 2, 3, 4, 5. \end{cases} \tag{26}$$

where ε is a small parameter, c_J are constants satisfying $\sum_J (c_J)^2 = 1$ and w_i^J are eigenvectors enumerated by the index J, $B_i{}^j w_j^J = \theta^J w_i^J$, with $\theta^J < 0$.

First fixed point at finite λ

θ^I	w_λ	w_{v_1}	w_{v_2}	w_{v_3}	w_{u_s}
-0.3416	7.159×10^{-9}	-0.9999	-2.323×10^{-3}	4.48×10^{-5}	3.411×10^{-4}
-0.06495	8.536×10^{-6}	-0.9909	0.09028	-0.05745	0.08206

Table: Stability matrix eigenvectors with negative eigenvalues for the first fixed point

We choose constants c_J in the initial conditions on the unit circle

$$c_1 w^1 + c_2 w^2 = \cos\varphi\, w^1 + \sin\varphi\, w^2 \,, \quad \varphi \in [0, 2\pi) \,. \tag{27}$$

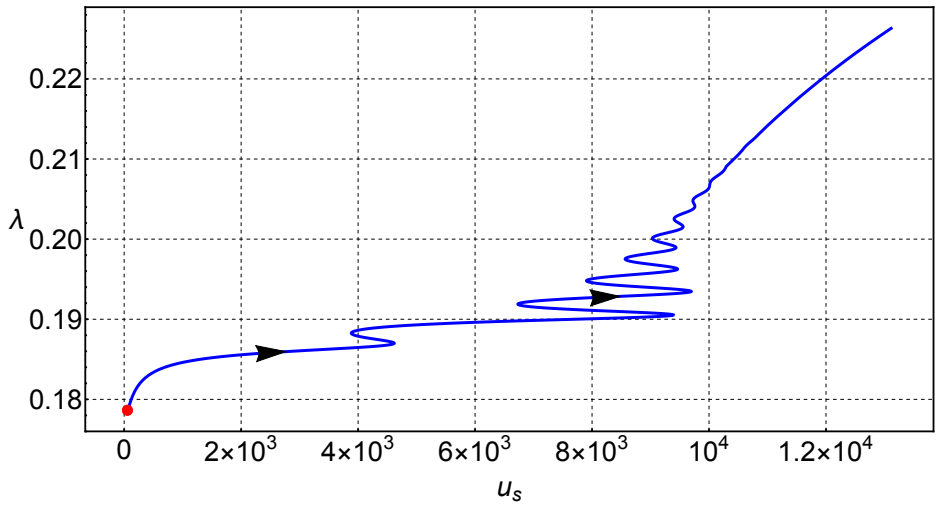

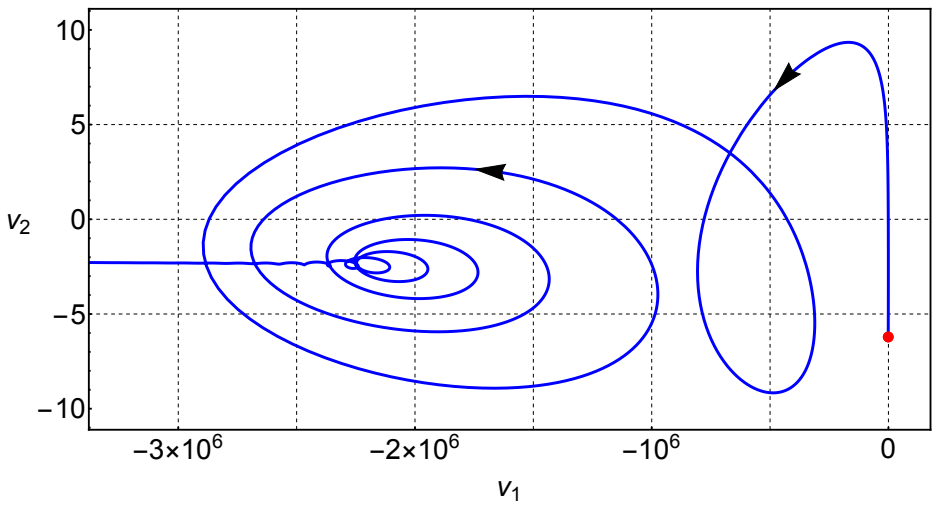

Second fixed point at finite λ

θ^I	w_λ	w_{v_1}	w_{v_2}	w_{v_3}	w_{u_s}
-0.06504	2.511×10^{-6}	1.339×10^{-3}	7.199×10^{-3}	-3.395×10^{-4}	0.9999

Table: Stability matrix eigenvectors with negative eigenvalues for the second fixed point

There are only two RG trajectories corresponding to different signs of c_1. Projections of one of them are depicted on the plots

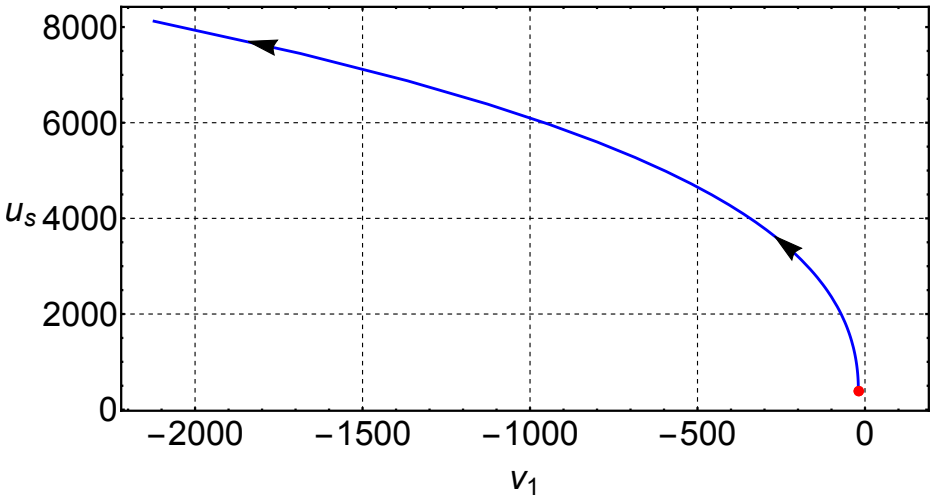

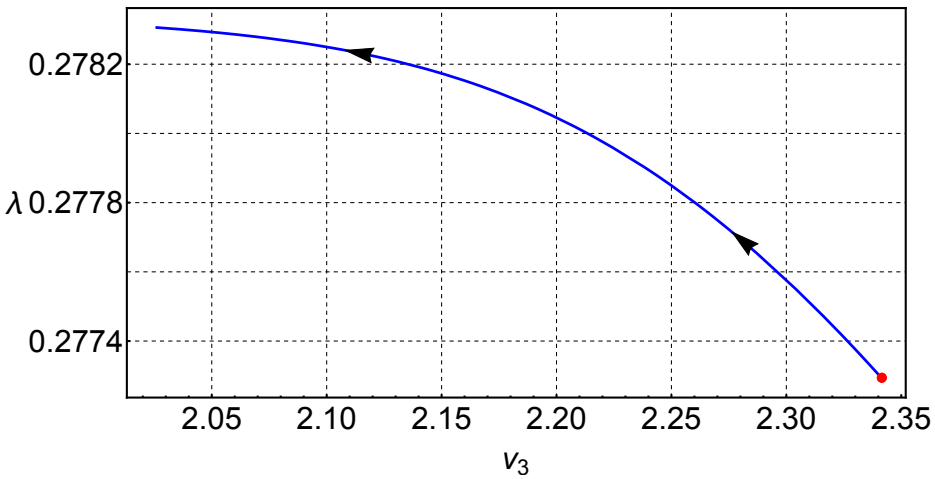

RG flows from fixed points at $\lambda = \infty$

Stability matrix

Stability matrix eigenvalues in variables (v_a, u_s, ϱ) with $\varrho = 1$

№	θ^1	θ^2	θ^3	θ^4	θ^5
1	1.154	-1.235	-0.2734 $\pm$ 0.2828 i		0.9825
2	0.5302	-71.95 $\pm$ 5.134 i		-0.3207	12.35
3	0.3970	-64.72 $\pm$ 0.6149 i		0.3012	10.77
4	-0.01334	-0.3436	-0.09353	0.2200 $\pm$ 0.1806 i	
5 (A)	-0.01414	-0.06998	0.06569	0.2565	0.3204
6 (B)	-0.01515	0.0924 $\pm$ 0.2890 i		0.3079	0.6032
7	-0.01516	-1.722	-0.3324 $\pm$ 0.3289 i		0.1328
8	-0.01517	-0.3657	0.4340 $\pm$ 0.4849 i		1.326

Table: Eigenvalues θ^I of the stability matrix for the fixed points with infinite λ.

From A to B

Eigen-vector	w_ϱ	w_{v_1}	w_{v_2}	w_{v_3}	w_{u_s}
$A1$	0.0423	-0.0398	5.25×10^{-3}	5.57×10^{-3}	0.998
$A2$	0	-0.115	-0.224	0.0480	-0.967
$B1$	2.19×10^{-5}	-0.999	1.87×10^{-5}	5.69×10^{-6}	0.0162

Table: Eigenvectors of the stability matrix with negative eigenvalues for the fixed points A and B.

First we build the trajectory flowing from point A along the eigenvector $A2$. Since this vector has zero ϱ-part, the trajectory stays in the hyperplane $\varrho = 1$.

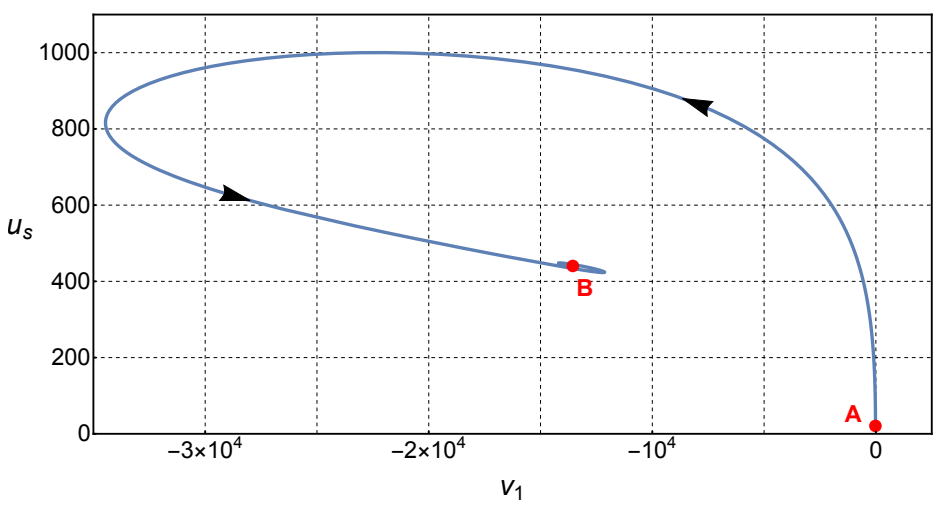

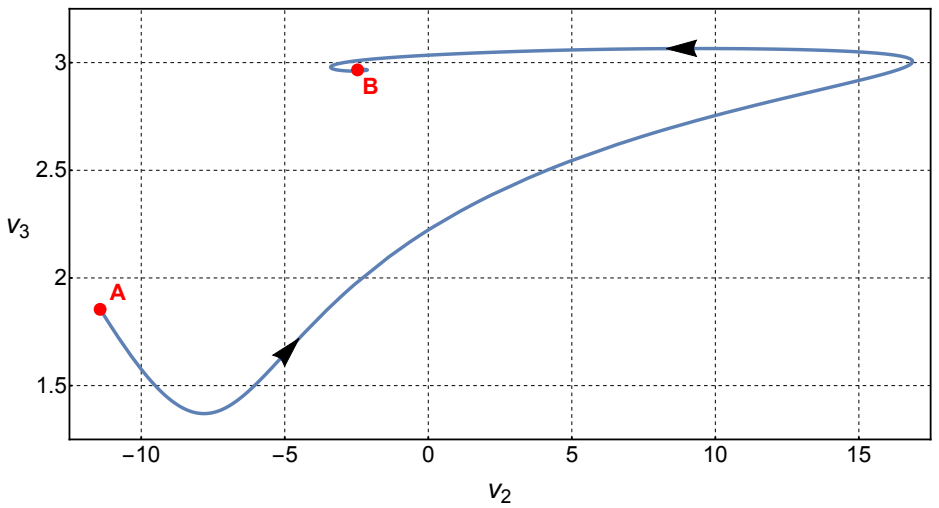

From B to $\lambda \to 1^+$

Point B has a unique repulsive direction, pointing away from the $\varrho = 1$ hyperplane. This gives rise to two RG trajectories, depending on the sign of c_{B1} in the initial conditions.

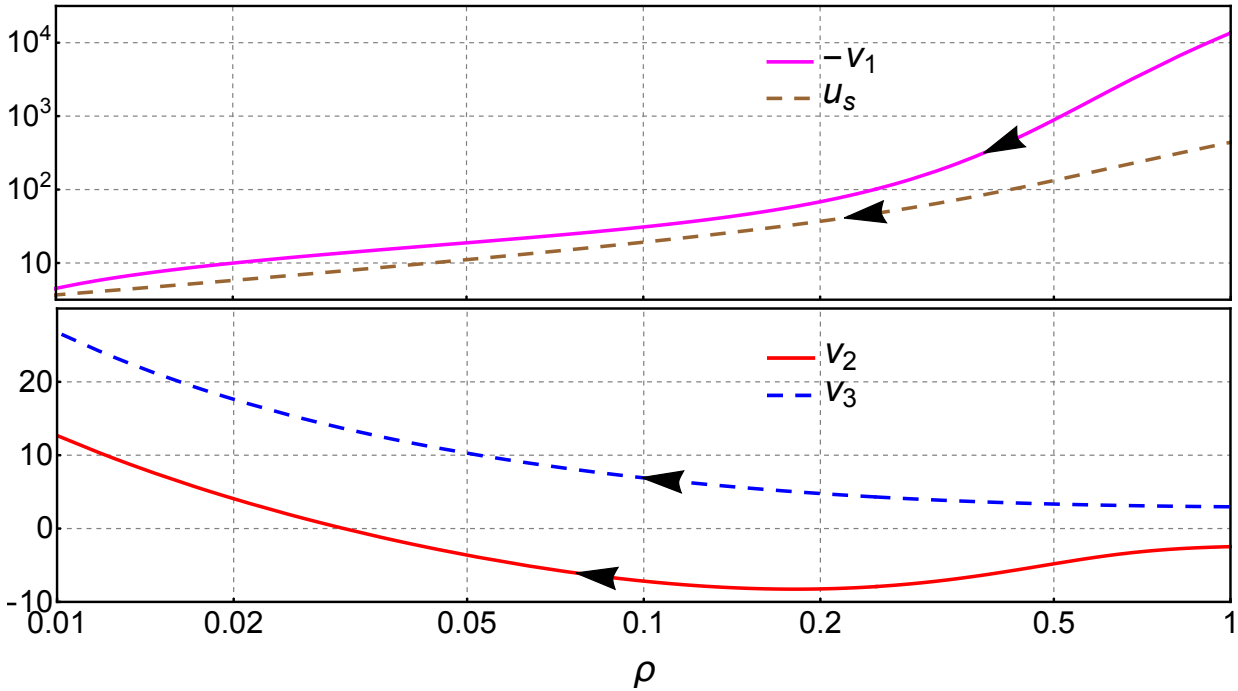

Figure: The couplings (u_s, v_a) as functions of ϱ along the RG trajectory from the fixed point B to $\varrho = 0$ $(\lambda \to 1^+)$. Arrows indicate the flow from UV to IR.

From B to $\lambda \to 1/3^-$

Point B has a unique repulsive direction, pointing away from the $\varrho = 1$ hyperplane. This gives rise to two RG trajectories, depending on the sign of c_{B1} in the initial conditions.

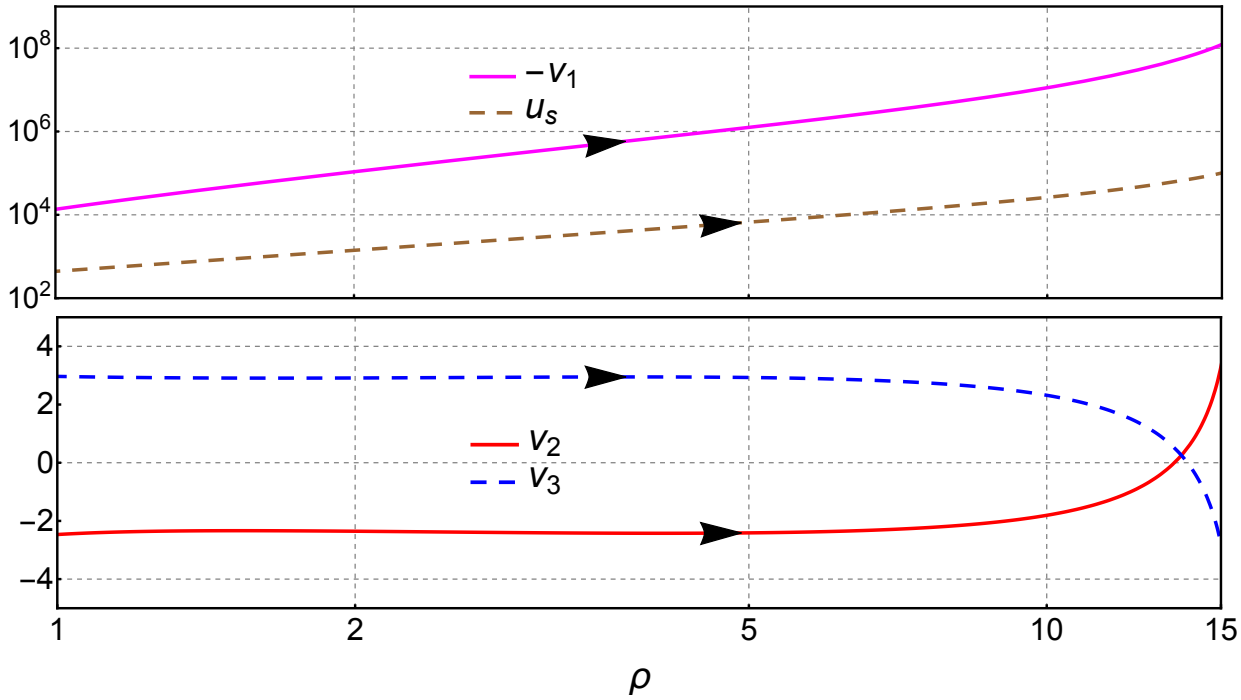

Figure: The couplings (u_s, v_a) as functions of ϱ along the RG trajectory from the fixed point B to $\varrho = 0$ ($\lambda \to 1/3^-$). Arrows indicate the flow from UV to IR.

Back to flows from A

We consider a general linear combination of vectors $A1$ and $A2$ in the initial condition (26) at the point A

$$c_{A1}w^{A1} + c_{A2}w^{A2} = \cos\varphi_A w^{A1} + \sin\varphi_A w^{A2} \ , \tag{28}$$

where $\varphi_A \in [0, 2\pi)$.

A chart illustrating global properties of the RG trajectories flowing from the fixed point A along different directions parametrized by the angle φ_A. Parameter $\delta \ll 1$.

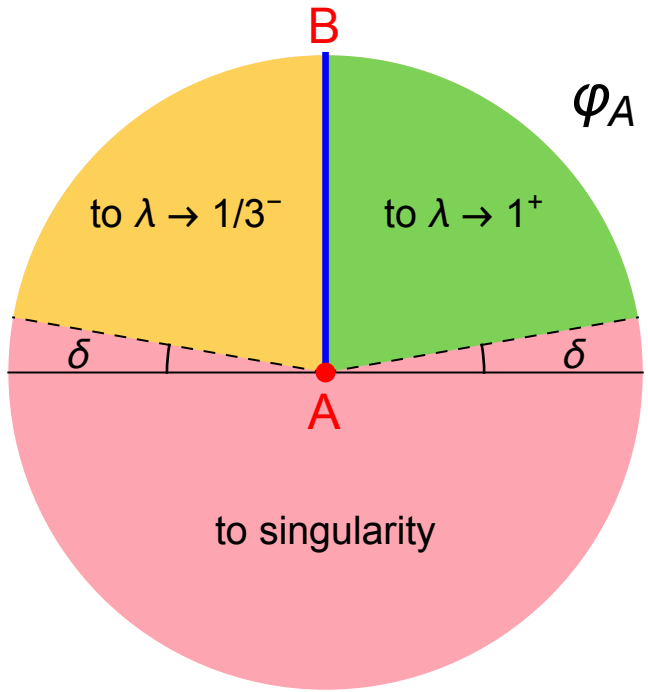

Trajectories emanating from the fixed point A cover the whole range of λ in the unitarity domain:

$$\lambda < 1/3 \quad \text{or} \quad \lambda > 1 \ .$$

From A to $\lambda \to 1^+$ and $\lambda \to 1/3^-$

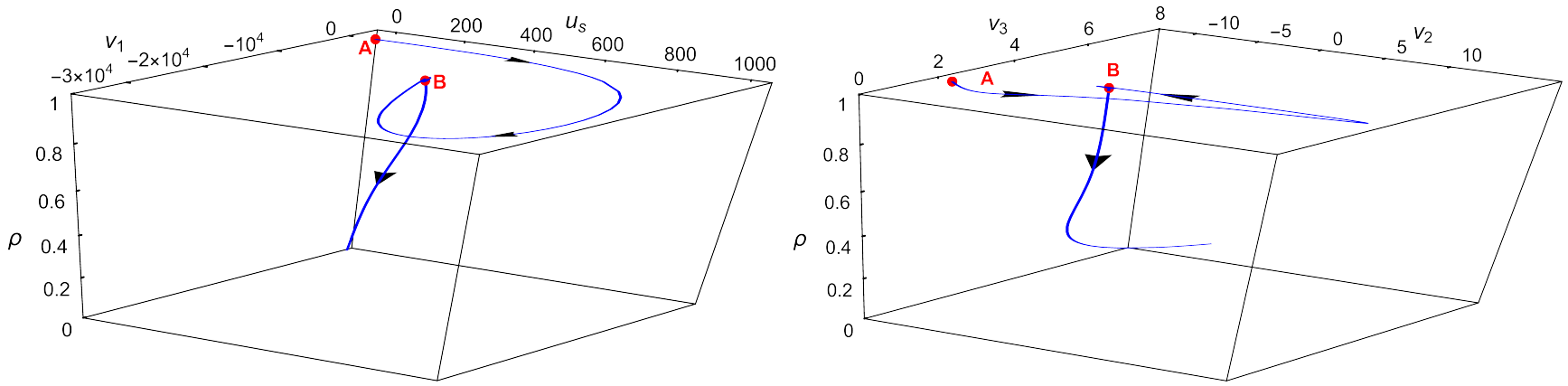

Figure: RG flows from the fixed point A to $\lambda \to 1^+$ ($\varrho \to 0^+$).

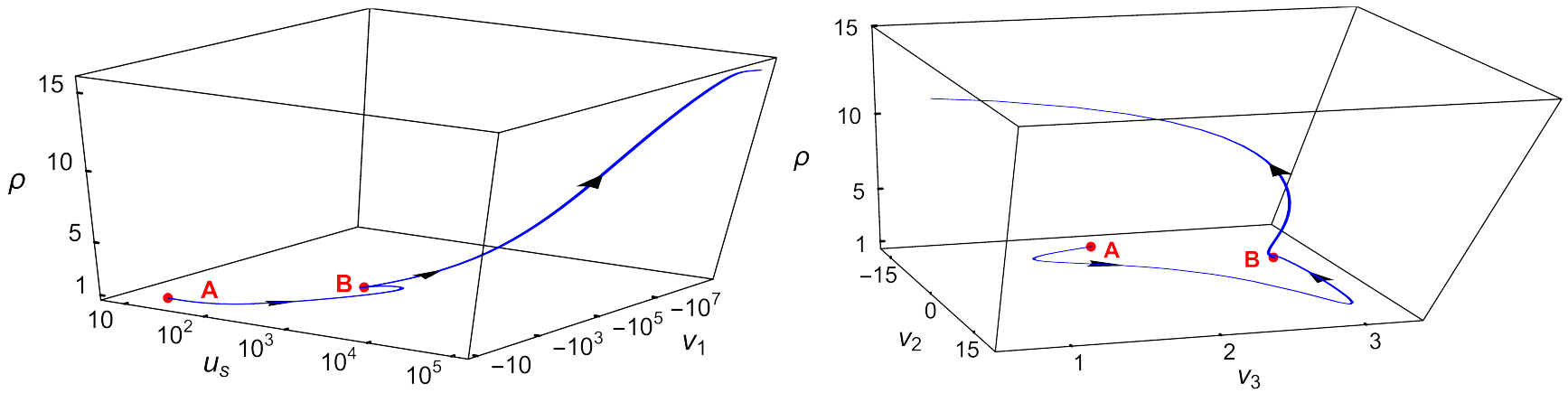

Figure: RG flows from the fixed point A to $\lambda \to 1/3^-$ ($\varrho \to \infty$).

From A to $\lambda \to 1^+$: the behaviour of $\mathcal{G}$

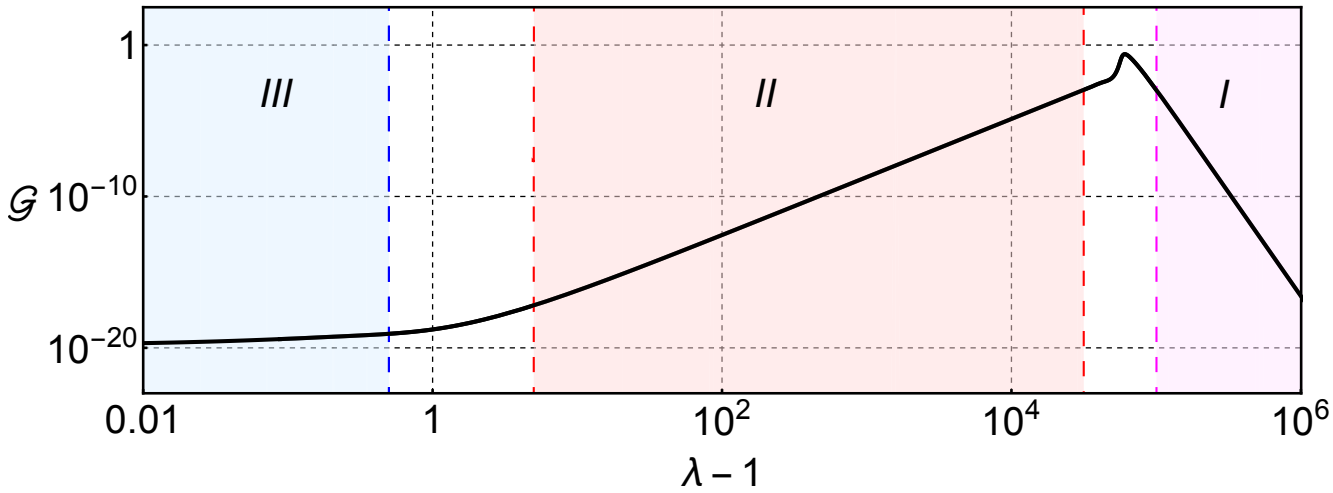

Figure: Behaviour of $\mathcal{G}$ as a function of $(\lambda - 1)$ along an RG trajectory connecting the point A to $\lambda \to 1^+$. In regions I, II and III the dependence is well described by the power law $\mathcal{G} \propto (\lambda - 1)^k$ with $k_I = -13.69$, $k_{II} = 3.84$, $k_{III} \approx 0.37$.

In the vicinity of $\lambda = 1$, we obtain the following scalings of the couplings

$$\mathcal{G}\,\big|_{\lambda\to 1} \propto (\lambda - 1)^{17/448}, \quad u_s\,\big|_{\lambda\to 1} \propto (\lambda - 1)^{241/448}, \quad v_a\,\big|_{\lambda\to 1} \propto \frac{1}{\lambda - 1}\,. \quad (29)$$

This means that all beta functions diverge when $\lambda \to 1$.

From A to $\lambda \to 1/3^-$: the behaviour of $\mathcal{G}$

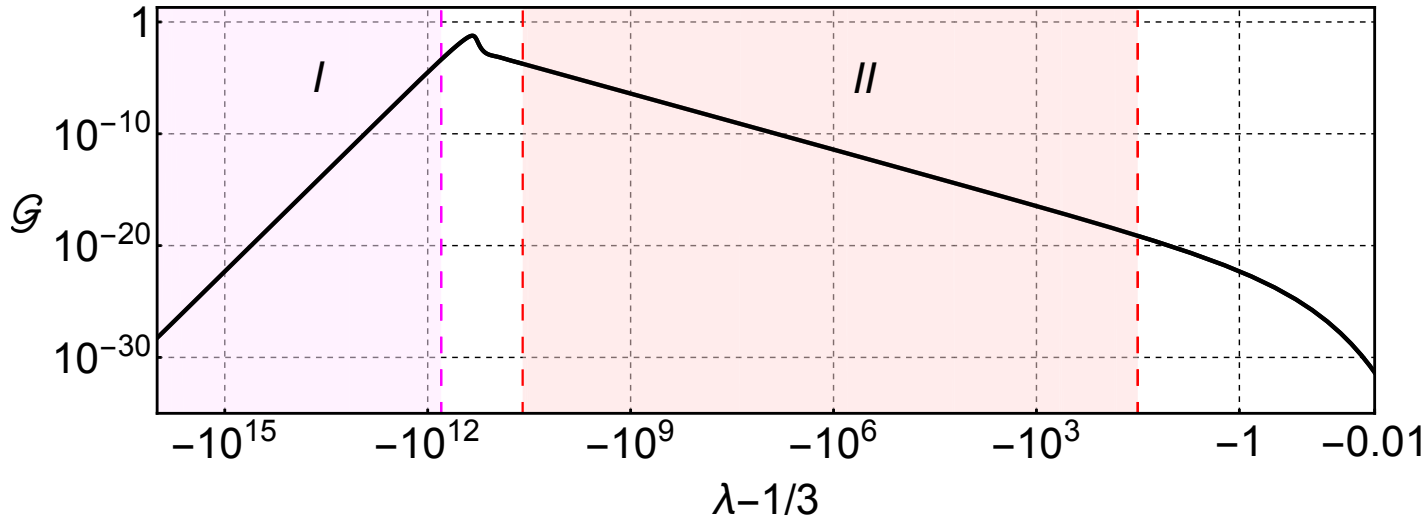

Figure: Behaviour of $\mathcal{G}$ as a function of $(\lambda - 1/3)$ along an RG trajectory connecting the point A to $\lambda \to 1/3^-$. In regions I and II the dependence is well described by the power law $\mathcal{G} \propto (\lambda - 1/3)^k$ with $k_I = -13.69$, $k_{II} = 3.84$.

Lorentz breaking scale M_{LV}

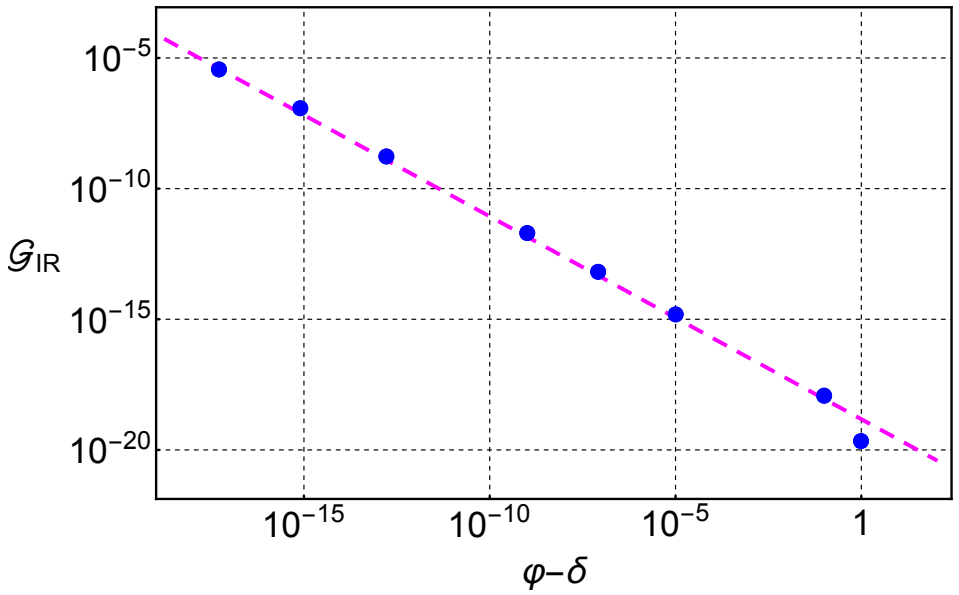

Dependence of the IR value of the gravitational coupling

$$\mathcal{G}_{IR} = \mathcal{G}_{IR}(\lambda)\big|_{\lambda=1.01} \tag{30}$$

on the initial direction of the trajectory at the point A. Dots show the numerical result while dashed line is the fit

$$\begin{aligned} &\mathcal{G}_{IR} = \mathcal{G}^{(0)}_{IR}\,(\varphi_A - \delta)^{\alpha}, \\ &\alpha = -\kappa_{II}\cdot\frac{\theta^1}{\theta^2} = -0.776\ , \end{aligned} \tag{31}$$

Recalling that $G = M_{Pl}^{-2}$, $\mathcal{G} = G/\sqrt{\nu_5}$ and $M_{LV} = \nu_5^{-1/4}$ we obtain a hierarchy

$$\frac{M_{LV}}{M_{Pl}} = \sqrt{\mathcal{G}_{IR}} \ll 1\ . \tag{32}$$

Such hierarchy could lead to strong suppression of Lorentz violating effects in gravity at low energies: M. Pospelov, Y. Shang, Phys.Rev.D 85, 105001 (2012)

Conclusions and outlook

- All the fixed points of RG flow were found.
- Trajectories flowing out asymptotically free UV fixed points analyzed. Most of them run into singularity.
- It's nontrivial that there exist two families of trajectories which cover the whole range of λ in the unitarity domain.
- In the IR domain, trajectories of one of the families run to the region with $\lambda \to 1^+$, i.e. towards GR value of the coupling λ.
- It would be interesting to understand whether non-projectable Hořava gravity possesses similar RG fixed points, trajectories and hierarchy.

The research was supported by the Russian Science Foundation grant № 23-12-00051.